Minimalist turbulent boundary layer model

L. Moriconi
Instituto de Física, Universidade Federal do Rio de Janeiro, C.P. 68528, 21945-970 Rio de Janeiro, RJ, Brazil
(Received 5 September 2008; published 6 April 2009)

We discuss an elementary model of a turbulent boundary layer over a flat surface given as a vertical random distribution of spanwise Lamb-Oseen vortex configurations placed over a nonslip boundary-condition line. We are able to reproduce several important features of realistic flows, such as the viscous and logarithmic boundary sublayers, and the general behavior of the first statistical moments (turbulent intensity, skewness, and flatness) of the streamwise velocity fluctuations. As an application, we advance some heuristic considerations on the boundary layer underlying kinematics that could be associated with the phenomenon of drag reduction by polymers, finding a suggestive support from its experimental signatures.

DOI: 10.1103/PhysRevE.79.046306 PACS number(s): 47.27.nb, 47.27.De

I. INTRODUCTION

Turbulent boundary layers have been a central topic of interest in fluid dynamic research for long years [1,2]. Nevertheless their obvious technological importance, a satisfactory description of the physical mechanisms which underlie the boundary velocity fluctuations remains elusive to date. As the result of intensive computational and experimental efforts carried out mainly along the last two decades, it is by now clear that the turbulent boundary layer is the stage for the production and the complex interaction of coherent structures [3], a fact that was formerly anticipated by Theodorsen [4] and Townsend [5].

Standard phenomenological formulations of the turbulent boundary layer problem aim at solving self-consistent equations for the expectation values of velocity and the Reynolds stress tensor components, which are relevant quantities in engineering applications [2,6]. However, the simulation of turbulent flows close to boundaries is plagued with well-known difficulties. The closure procedures which take into account up to second-order statistical moments invariably fail when inserted in practical computational fluid dynamic packages. The ultimate reason for such failure is that the intermittent boundary fluctuations originated from coherent structures break, in general, the closure assumptions. At the very conception of the usual models, no fundamental role is given to the whole boundary layer zoo of coherent structures, such as streamwise and hairpin vortices, low-speed streaks, etc. It is an unsettled question, for instance, whether a structural derivation of the Prandtl-von Karman logarithmic law of the wall is viable. In this sense, turbulent boundary layer modeling is a difficult problem of statistical physics, analogous to the derivation of thermodynamic equations of state from a molecular starting point. Vortex methods have been around for some time in turbulence modeling [7], but their application to turbulent boundary layer phenomena is still very open, which is somewhat surprising, since an initial discussion may be traced back to 1982 with Perry and Chong [8].

We are interested to develop here a *kinematical* picture of some important aspects of the turbulent boundary layer phenomenology, all of them related to coherent structure fluctuations. We compute a set of general profiles for statistical moments of the streamwise component of velocity, clearly supported by observational results. Our work differs from previous attempts [8–12] essentially in its qualitative scope, stronger simplifying assumptions, specific coherent structure modeling (the vortex-dipole model to be discussed below), and the analysis of higher-order statistics for the streamwise velocity fluctuations. Let us emphasize that we do not seek, at the present level of mathematical treatment, sharp quantitative agreement with experiments or a detailed comparison to known boundary layer models.

This paper is organized as follows. In Sec. II we discuss the modeling principles which will be applied, in Sec. III, to the computation of velocity and velocity-moment profiles. In Sec. IV, the model is adapted to describe statistical signatures found in polymer drag-reduced flows. In Sec. V we summarize our findings and point directions of further research.

II. MODEL

Our focus is on the streamwise fluctuations of the velocity field. Let us assume that close enough to the wall these fluctuations are mostly due to the flow generated by hairpin vortices [13–15], like the one depicted in Fig. 1, momentarily located in the surroundings of the measurement position. The main contribution to streamwise fluctuations would come from the spanwise sector of hairpin vortices (also called "hairpin's head"), while subdominant contributions would be related to their necks and legs. This picture is in fact suggested by recent particle image velocimetry (PIV) experiments performed by Wu and Christensen [14].

It is clear that turbulent boundary layers contain much more than streamwise fluctuations. By neglecting normal to the wall and spanwise fluctuations, we are necessarily addressing a kinematical description, which relies on phenomenological inputs.

In order to model streamwise fluctuations of velocity, it is natural to replace the hairpin vortex with a simpler and more mathematically tractable structure, which we take to be a spanwise Lamb-Oseen vortex, an exact and nonstationary solution of the Navier-Stokes equations, described in cylindrical coordinates as

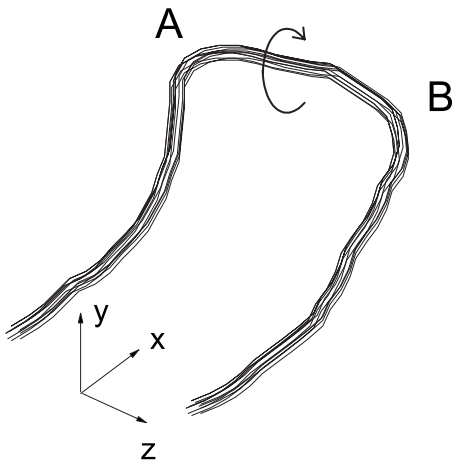

FIG. 1. A hairpin vortex which propagates along the positive x direction. Streamwise fluctuations of the velocity field, associated to the passage of the hairpin vortex, are due essentially to the flow generated by its spanwise sector, which lies between points A and B. The curved arrow indicates the vorticity orientation.

$$u_\theta(r) = \frac{\Gamma}{2\pi r}[1 - \exp(-r^2/2r_c^2)], \tag{2.1}$$

where Γ is the total circulation around the vortex and $r_c^2 = 2\nu t$ is the squared vortex core radius at time t, defined in terms of the kinematical viscosity ν. Other alternatives, as the Rankine vortex, for instance, would be well suited for our modeling purposes. The time dependence of the Lamb-Oseen vortex, however, is an interesting ingredient, as it will be discussed below.

Of course, Eq. (2.1) solves the fluid equations of motion in the absence of boundaries, so Eq. (2.1) is just a rough approximation to a real vortex parallel to the wall. In our modeling definitions, we postulate that the symmetry axis of the vortex lies in the plane (henceforth designed the "measurement plane") that contains the measurement point and is normal to the wall. We assume, then, that at equally spaced time intervals, a given vortex is replaced with another one, at a random distance y from the wall, with some prescribed probability distribution function (pdf) $\rho(y)$. The profile of the vertical random distribution of vortices should be related somehow to the statistical properties of mixing in the boundary layer. However, as vertical velocity fluctuations have been completely neglected, boundary layer mixing is, in fact, not reproduced in our kinematical model.

Borrowing ideas from two-dimensional fluid mechanics, a mirror vortex is presented "below the wall," so that streamlines do not cross the material surface. Furthermore, in order not to completely neglect the nonslip boundary condition, some improvement is attained if we make the velocity field to vanish at the intersection of the measurement plane with the wall. For this purpose, an external homogeneous velocity field is superimposed to the field generated by the vortex dipole. These definitions are shown in Fig. 2.

An interpretation of the time dependence in Eq. (2.1) is in order. The time variable t is taken to be the total time elapsed since the hairpin vortex was created at the wall. This assumption, however, is not of great help if there is no way to relate the vortex vertical position y to the time t. To solve this problem, at least in a phenomenological fashion, we find inspiration in the scaling structure of the *laminar* boundary layer over a flat surface. It is well established, and analytically predicted by the Blasius solution, that the laminar boundary layer thickness grows with the distance from the leading edge as $\delta \sim \sqrt{x}$. This result can be understood in elementary terms as the fact that any small perturbation which is transported along the main direction of the flow (say, the horizontal one) follows a diffusive drift along the vertical direction. An analogy to the context of turbulent boundary layers can be drawn, replacing words such as "perturbations" with "coherent structures" and "molecular viscosity" with "eddy viscosity." Actually, hairpin vortices are observed to grow in size as they get farther from the surface [15]. Therefore, we suppose that at time t a diffusionlike relation $t \sim y^2$ holds and the vortex core radius can be written as $r_c = ay$ in Eq. (2.1), where a plays the role of a phenomenological parameter in the turbulent boundary layer modeling [16].

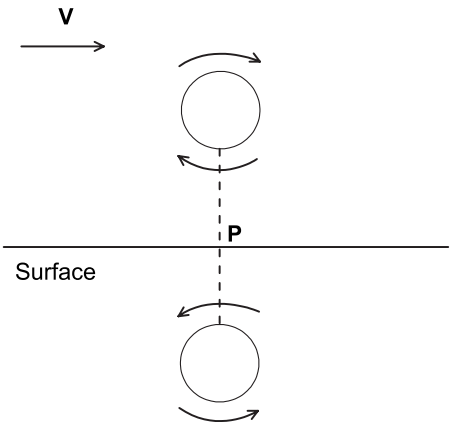

FIG. 2. The vortex-dipole construction. The dashed line is contained in the measurement plane. The upper plane vortex is the "real" one, while the other is its mirror image. A uniform background flow with velocity V is superimposed to the velocity field produced by the vortices, so that P is a stagnant point.

The flow depicted in Fig. 2 is assumed to describe a boundary layer with no pressure gradient. This is so because the velocity field is symmetric under reflections on the measurement plane. Pressure gradients are probably related to the flow induced by the whole gas of hairpin's vortices, appearing, therefore, as a "many-body" effect.

We are now ready to work out a few relevant equations. Suppose that the Lamb-Oseen vortices are centered at y and $-y$. The streamwise velocity field vanishes at point P in Fig. 2. Once the resulting streamwise velocity is given as the sum of three contributions (the external, the real, and the mirror vortex velocity fields), we get, using Eq. (2.1),

$$0 = V - \frac{\Gamma}{\pi y}[1 - \exp(-1/2a^2)]. \tag{2.2}$$

The above equation holds for any y only if the total circulation Γ is a y-dependent quantity. We find

$$\Gamma(y) = \frac{\pi V y}{1 - \exp(-1/2a^2)}. \tag{2.3}$$

It is a straightforward task to evaluate expectation values of general y-dependent functionals $F=F[u(y)]$ of the streamwise velocity field. It follows that

$$\langle F[u(y)]\rangle = \int_0^\infty dy'\ \rho(y')F[u(y,y')], \tag{2.4}$$

where the "two-point velocity"

$$u(y,y') = V + \frac{\Gamma(y')}{2\pi(y-y')}\{1 - \exp[-(y-y')^2/2a^2y'^2]\} - \frac{\Gamma(y')}{2\pi(y+y')}\{1 - \exp[-(y+y')^2/2a^2y'^2]\} \tag{2.5}$$

is nothing but the velocity field at y when the Lamb-Oseen vortices are placed at y' and $-y'$.

III. SUBLAYERS AND HIGHER-ORDER STATISTICS

We have applied Eq. (2.4) for a set of velocity functionals, comparing the y-dependent profiles so obtained with experimental results, as discussed below. As input parameters, we take $a=1.0$ and $V=1.0$ (i.e., the streamwise velocity is computed in units of the external velocity V). We use the pdf

$$\rho(y) = \frac{2b}{\pi(y^2+b^2)} \tag{3.1}$$

with $b=1.0$ to model fluctuations of the vortex's height above the surface. It is important to note that the choice of the Lorentzian distribution (3.1), although arbitrary, is by no means restrictive. We have checked out that smoothly decaying distributions lead to similar conclusions if one is indeed interested in a *qualitative* understanding of turbulent boundary layer fluctuations.

A. Viscous and logarithmic layers

The mean streamwise velocity is obtained from the expectation value of $F[u(y)]=u(y)$. The overall profile is shown in Fig. 3, which interpolates between zero velocity at the wall and unit velocity at infinity. Even though $u(y)$ seems to give a reasonable profile for the interval $0\le y<\infty$, the model does not apply to the outer layer because of the stronger interactions between coherent structures and also for the high intermittency produced by the random entrainment of external laminar flow that takes place in that region.

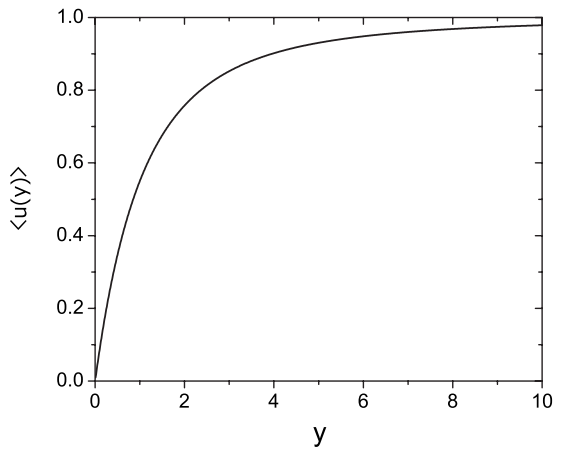

FIG. 3. The mean streamwise velocity.

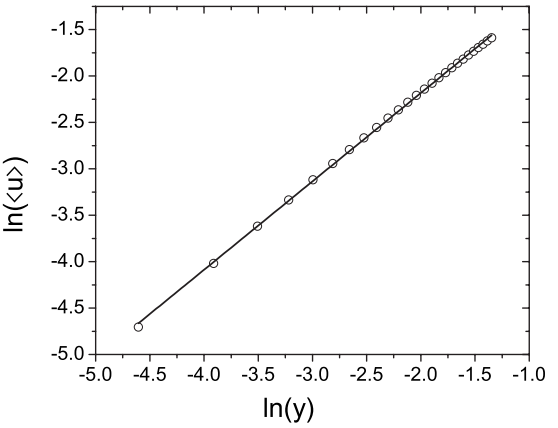

FIG. 4. The viscous layer, verified in the range $0.01\le y\le 0.25$. The straight line has slope of 0.95.

In Figs. 4 and 5, viscous and logarithmic layers are clearly noticed for certain ranges of vertical distances. The excellent fit of the data to the straight line in Fig. 5 is given by $\langle u(y)\rangle = 0.31\ \ln(y) + 0.55$. The numerical coefficients have precision of 0.1%. Observe that a purely dimensional argument yields $u(y)=Vf(y/b)$ in our particular model. Therefore, the numerical verification of a logarithmic layer forces us to identify the effective external velocity V to the friction velocity, up to numerical factors. We may conjecture, thus, that the friction velocity is "what is left" when a few dominant vortical structures near the wall are removed. In other words, the friction velocity can be interpreted here as a "mean field," while fluctuations are modeled by isolated vortex dipoles.

B. Higher-order statistics

Let $F_n[u(y)] \equiv [u(y) - \langle u(y)\rangle]^n$. We have

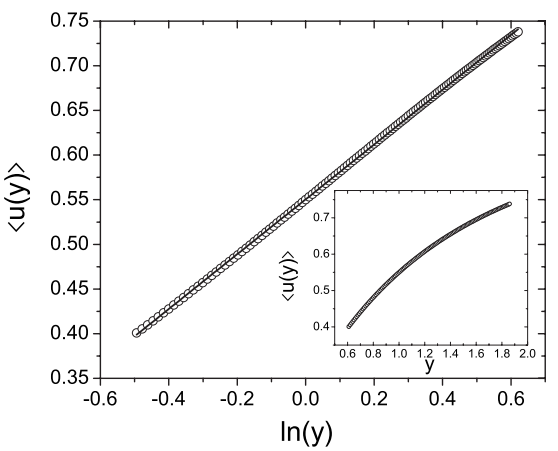

FIG. 5. The logarithmic layer, verified for $0.6\le y\le 1.85$. The inset shows the same data plotted in linear scales.

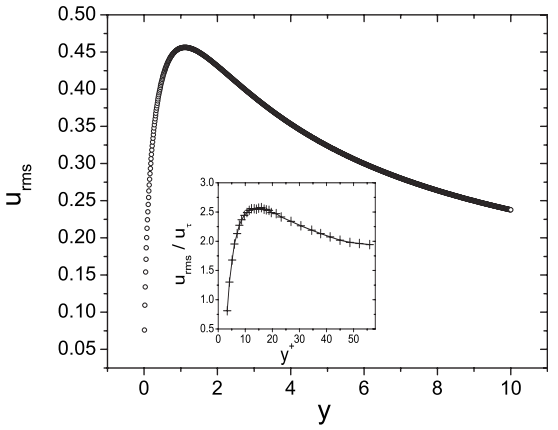

FIG. 6. The $u_{\rm rms}$ velocity. The inset shows the experimental measurements of $u_{\rm rms}$ by Lorkowski [17].

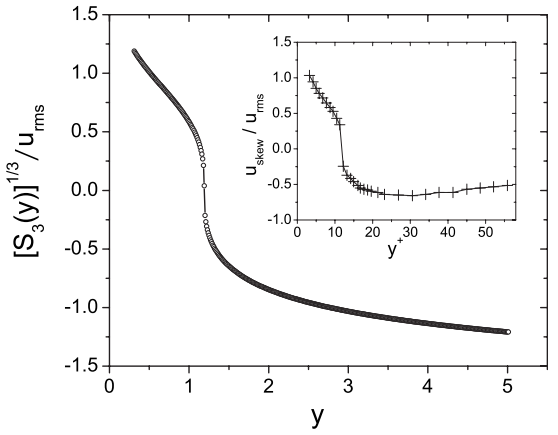

FIG. 7. The skewness for $0.3 \leq y \leq 5.0$. The inset shows the experimental measurements of $S_3(y)^{1/3}/u_{\rm rms}$ by Lorkowski [17].

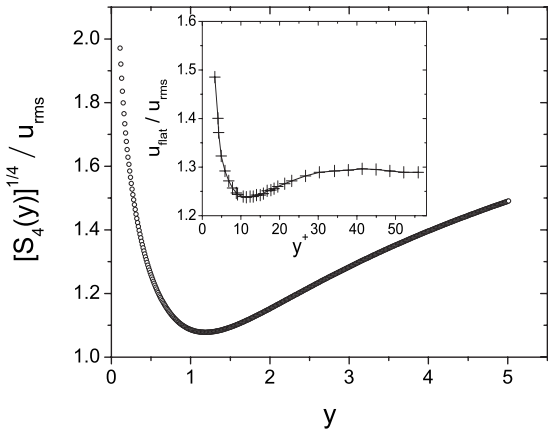

FIG. 8. The flatness for $0.1 \leq y \leq 5.0$. The inset shows the experimental measurements of $S_4(y)^{1/4}/u_{\rm rms}$ by Lorkowski [17].

$$u_{\rm rms} = \sqrt{\langle F_2[u(y)]\rangle} \tag{3.2}$$

and the hyperflatness functions $S_n(y)$ given by

$$S_n(y) = \frac{\langle F_n[u(y)]\rangle}{\sqrt{\langle F_2[u(y)]\rangle^n}}. \tag{3.3}$$

Fine measurements of turbulent boundary layer fluctuations for S_3 (skewness) and S_4 (flatness or kurtosis), which can resolve the region very close to the surface, are reported in Ref. [17]. As we can see from Figs. 6–8, there is a clear qualitative agreement with observations. In particular, the abrupt sign-changing transition of skewness is remarkably reproduced by the vortex-dipole model.

IV. DRAG REDUCTION BY POLYMERS

The phenomenon of drag reduction by polymers [18,19] is a long-standing puzzle of non-Newtonian fluid mechanics. The broad picture is that dissipation is attenuated due to the interaction of polymers with the coherent structures created near walls.

Recent PIV experiments in flows with dilute polymers have shown that vorticity fluctuations—and probably coherent structures—are suppressed at some point above the surface in turbulent boundary layers [20]. Also, by about the same time, interesting signatures of drag reduction have been found in the profiles of $u_{\rm rms}(y)$ and $S_3(y)$ in connection with polymer dilution [21]. An additional peak is observed for $u_{\rm rms}(y)$, while the skewness $S_3(y)$ shows further sign-changing transitions.

The vortex-dipole model allows us to relate these apparently distinct features of drag reduction by polymers. Coherent structure suppression can be naturally accounted for by changing the form of the vortex pdf $\rho(y)$. We take, for instance, a distribution which is uniform for $0 \leq y \leq c$, but vanishes for $y > c$, that is,

$$\rho(y) = c^{-1}[\theta(y) - \theta(y-c)], \tag{4.1}$$

where $\theta(y)$ is the Heaviside function. Therefore, we suppose that no vortex is found for $y > c$, as the result of polymer

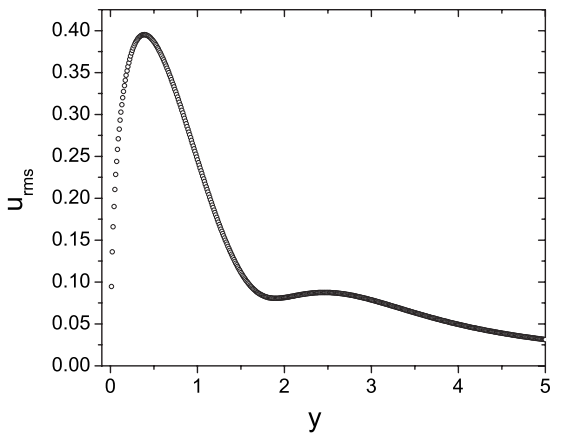

FIG. 9. The $u_{\rm rms}$ velocity, as affected by coherent structure suppression, for $0.01 \leq y \leq 5.0$. An additional peak is observed at $y \simeq 2.5$.

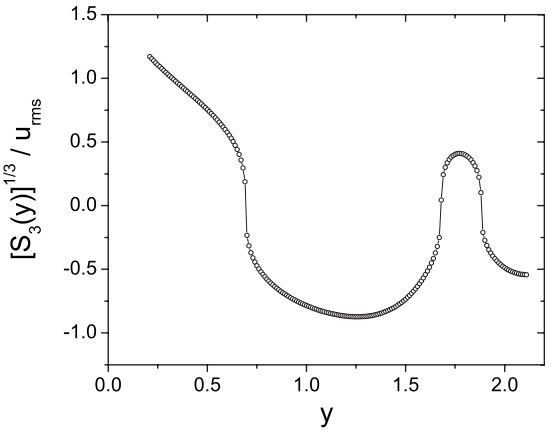

FIG. 10. The skewness, as affected by coherent structure suppression, for $0.2 \leq y \leq 2.1$. Note the additional sign-changing transitions that take place within $1.5 < y < 2.0$.

interactions. Setting $c=1.0$ and keeping the previous definitions of a, b, and V, we get the results shown in Figs. 9 and 10, which are in striking correspondence with real profiles [21].

V. CONCLUSIONS

We have presented an elementary model of a turbulent boundary layer, focusing our attention on the streamwise fluctuations of velocity induced by hairpin vortices. The model's main scope is to provide qualitative insights on the velocity and hyperflatness profiles. The profiles of skewness and flatness of usual turbulent boundary layers as well as certain statistical signatures of the phenomenon of drag reduction by polymers have been theoretically reproduced by means of vortex methods.

However, the present model does not take into account dynamical aspects of the turbulent boundary layer phenomenology, which become important if the interest is shifted toward *predictive* quantitative results (e.g., a determination of the von Karman constant). An essential improvement, along the above lines, would be to introduce a pair of streamwise vortex configurations with opposite vorticity as a way to mimic hairpin legs. In this way, one could try to compute the shear stress and, thus, define in a self-consistent way the physical scales of length and velocity which are necessary for a statistical description of the inner boundary layer.

ACKNOWLEDGMENTS

This work was partially supported by CNPq and FAPERJ. I thank Atila Freire for several interesting discussions and for calling my attention to Refs. [8–11]. I also thank Katepalli Sreenivasan for kindly providing me a copy of Ref. [10].

[1] *One Hundred Years of Boundary Layer Research*, IUTAM Symposium, edited by G. E. A. Meier and K. R. Sreenivasan (Springer-Verlag, Berlin, 2004).
[2] H. Schlicthing and K. Gersten, *Boundary Layer Theory* (Springer-Verlag, Berlin, 2000).
[3] S. K. Robinson, Annu. Rev. Fluid Mech. **23**, 601 (1991).
[4] T. Theodorsen, *Mechanism of Turbulence*, Proceedings of the Midwestern Conference on Fluid Mechanics (Ohio State University, Columbus, OH, 1952).
[5] A. A. Townsend, *The Structure of Turbulent Shear Flow* (Cambridge University Press, Cambridge, England, 1976).
[6] S. B. Pope, *Turbulent Flows* (Cambridge University Press, Cambridge, England, 2000).
[7] D. I. Pullin and P. G. Saffman, Annu. Rev. Fluid Mech. **30**, 31 (1998).
[8] A. E. Perry and M. S. Chong, J. Fluid Mech. **119**, 173 (1982).
[9] A. E. Perry, S. M. Henbest, and M. S. Chong, J. Fluid Mech. **165**, 163 (1986).
[10] K. R. Sreenivasan, in *A Unified View of the Origin and Morphology of the Turbulent Boundary Layer Structure in Turbulence Management and Relaminarization*, edited by H. W. Liepmann and R. Narasimha (Springer-Verlag, Berlin, 1987).
[11] A. E. Perry and I. Marusic, J. Fluid Mech. **298**, 361 (1995).
[12] I. Marusic, Phys. Fluids **13**, 735 (2001).
[13] M. R. Head and P. Bandyopadhyay, J. Fluid Mech. **107**, 297 (1981).
[14] Y. Wu and K. T. Christensen, J. Fluid Mech. **568**, 55 (2006).
[15] R. J. Adrian, Phys. Fluids **19**, 041301 (2007).
[16] There is no strong argument to rule out a general anomalous diffusive ansatz $r_c = a y^{\alpha}$. We would not find, however, important qualitative departures for the results derived here.
[17] T. Lorkowski, Fluid Dynamics Research Laboratory, Massachusetts Institute of Technology Report No. FDRL TR 97-2, 1997, http: //raphael.mit.edu/pubsTechRep.html. (unpublished).
[18] B. A. Toms, *Proceedings of the International Congress on Rheology* (North-Holland, Amsterdam, 1949), p. 135.
[19] I. Procaccia, V. S. L'Vov, and R. Benzi, Rev. Mod. Phys. **80**, 225 (2008).
[20] C. M. White, V. S. R. Somandepalli, and M. G. Mungal, Exp. Fluids **36**, 62 (2004).
[21] M. Itoh, S. Tamano, K. Yokota, and M. Ninagawa, Phys. Fluids **17**, 075107 (2005).